Cone Calorimeter Combustion and Gasification Studies of Polymer Layered Silicate Nanocomposites

M. Zanetti,[†] T. Kashiwagi,[‡] L. Falqui,[§] and G. Camino*,[†]

Dipartimento di Chimica IFM, Università di Torino, Via Pietro Giuria 7, 10125 Turin, Italy, Fire Science Division, Building and Fire Research Laboratory, National Institute of Standards and Technology, Gaithersburg, Maryland 20899, and Istituto di Studi Chimico-Fisici di Macromolecole Sintetiche e Naturali, IMAG-CNR, Via De Marini 6, 16149 Genova, Italy

Received September 6, 2001. Revised Manuscript Received November 13, 2001

Polymer composites based on organically modified phyllosilicates (organoclay) and poly(ethylene-*co*-vinyl acetate) (EVA) were prepared by melt processing to study their combustion behavior. Their degrees of dispersion and intercalation spacings as determined by transmission electron microscopy (TEM) and X-ray diffraction (XRD) were typical of either a microcomposite or an exfoliated nanocomposite, depending on the type of organoclay. Combustion experiments showed that the microcomposite burns in the same way as pure EVA, whereas the heat release is reduced by 70−80% when nanocomposites with low silicate loadings (2−5%) are burned, because a protective charred ceramic surface layer is formed as a result of reassembly of the clay layers and catalyzed charring of the polymer. A chemical mechanism for this charring is proposed.

Introduction

Inorganic fillers are commonly added to polymers to increase their strength or impact resistance or to induce other properties such as electrical conductivity or reduced permeability to gases, e.g., oxygen and water vapor.[1] Their beneficial effects have been optimized in a new class of composite materials known as polymer-layered silicate nanocomposites (PLSNs),[2−5] which are hybrids composed of layered silicates (also called phyllosilicates) dispersed in a polymer matrix in the form of reticular layers of crystals about 1 nm thick and with a lamellar aspect ratio of between 100 and 1000. Prior to dispersion, the alkali cations in the interlayer galleries of the phyllosilicate are exchanged with organic cations such as *N*-alkylammonium to confer an organophilic character on the crystalline layers (organoclays). Nanodispersion of the organoclay is achieved by in situ polymerization, annealing diffusion, and melt processing,[6,7] which is the most appropriate technique for the industrial preparation of PLSNs of thermoplastic polymers. Two classes of PLSNs are obtained: intercalated nanocomposites, where the polymer chains are intercalated in the silicate galleries, and delaminated or exfoliated nanocomposites, where the delaminated silicate is uniformly dispersed in the matrix. Aspect ratios from 100 to 1000 result in polymers with high rigidities and heat stabilities, reduced gas permeabilities, and good transparencies with as little as 5−10 wt % silicate. PLSNs have been rendered even more attractive by recent demonstrations of their flame-retardant properties, namely, diminution of the heat release rate (HRR) peak, formation of protective char, and decrease in the rate of mass loss during combustion in a typical polymer material combustion test (cone calorimeter).[8−10] This paper describes the combustion behavior of a PLSN based on EVA, which is a polymer used for many applications in which flame-retardant properties are required, such as in electrical cables.

Experimental Section

Materials. The polymer (EVA) is Escorene UL00119 produced by Exxon, which is a poly(ethylene-*co*-vinyl acetate) with 19 wt % of vinyl acetate and a melt flow index of 0.65 g/10 min. The organoclay used to prepare the nanocomposite was Cloisite 30B (MMT30B), kindly provided by Southern Clay Products, Inc. It corresponds to a montmorillonite in which the ammonium cation on the clay contained a methyl group, tallow (containing 70, 25, 4, and 1 mol % of C18, C16, C14, and C12 carbon chains, respectively), and two hydroxyethyl groups (cationic exchange capacity of 90 mequiv/100 g). The organoclay used to produce the microcomposite was prepared

* Corresponding author: Prof. G. Camino, Università degli Studi di Torino, Dip. Chimica IFM, Via P. Giuria 7, 10125 Torino, Italy. Phone: +39-(0)11-670.75.57. Fax: +39-(0)11-670.78.55. E-mail: camino@silver.ch.unito.it.

[†] Università di Torino.

[‡] National Institute of Standards and Technology.

[§] Istituto di Studi Chimico-Fisici di Macromolecole Sintetiche e Naturali.

(1) Katz; H. S.; Milewski, J. W. In *Handbook of Fillers for Plastics*; Van Nostrand Reinhold: New York, 1987.

(2) Zanetti, M.; Lomakin, S.; Camino, G. *Macromol. Mater. Eng.* **2000**, *279*, 1.

(3) Giannelis; E. P. *Adv. Mater.* **1996**, *8*, 29.

(4) Zilg, C.; Dietsche, F.; Hoffman, B.; Dietrich, C.; Mülhaupt, R. In *Proceedings of Eurofiller '99*; 1999.

(5) Lagaly, G.; Pinnavaia, T. J. *Appl. Clay Sci.* **1999**, *15*.

(6) Vaia, R. A.; Jandt, K. D.; Kramer, E. J.; Giannelis, E. P. *Macromolecules* **1995**, *28*, 8080.

(7) Vaia, R. A.; Jandt, K. D.; Kramer, E. J.; Giannelis, E. P. *Chem. Mater.* **1996**, *8*, 2628.

(8) Gilman, J. W.; Jackson, C. L.; Morgan, A. B.; Harris, R.; Manias, E.; Giannelis, E. P.; Wuthenow, M.; Hilton, D.; Phillips, S. H. *Chem. Mater.* **2000**, *12*, 1866.

(9) Porter, D.; Metcalfe, E.; Thomas, M. J. K. *Fire Mater.* **2000**, *24*, 45.

(10) Zanetti, M.; Camino, G.; Mülhaupt, R. *Polym. Degrad. Stab.* **2001**, *24*, 413.

10.1021/cm011236k CCC: $22.00
Published on Web 01/29/2002

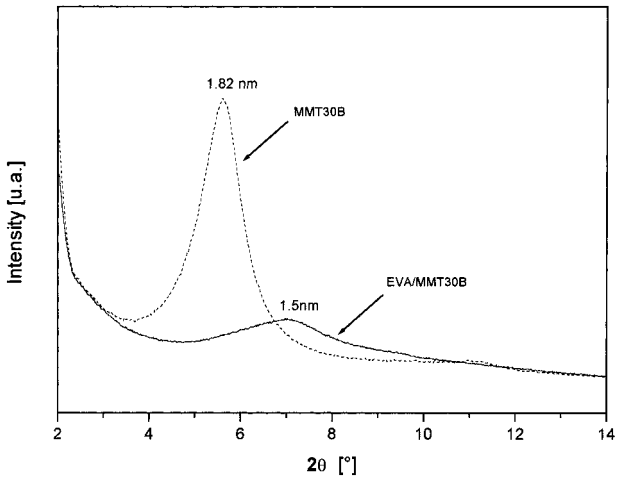

Figure 1. XRD patterns of montmorillonite exchanged with methyl, tallow, bis-2-dihydroxyethylammonium (MMT30B, dotted line) and EVA nanocomposite (EVA−MMT30B, solid line).

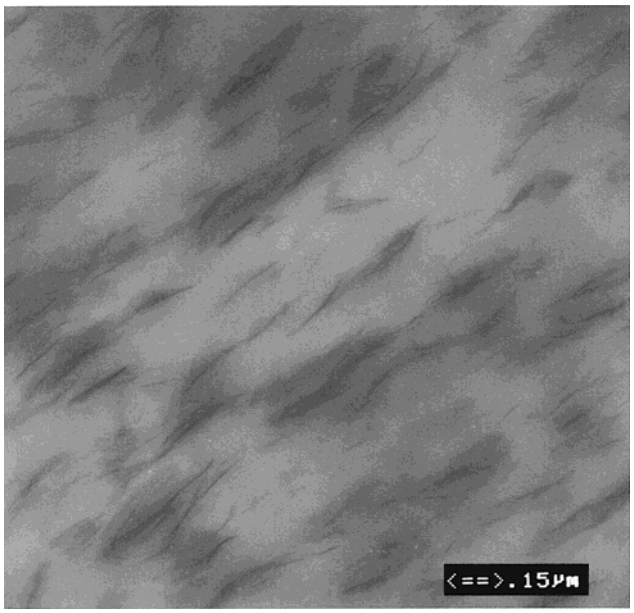

Figure 2. TEM of nanocomposites based on EVA filled with 5 wt % montmorillonite exchanged with methyl, tallow, bis-2-dihydroxyethylammonium (EVA−MMT30B).

at the Freiburger Materialforschungszentrum und Institute für Makromolekulare Chemie der Albert Ludwigs Universität Freiburg using the synthetic silicate Somasiftm ME100 (FH) (fluorohectorite like structure, from Co-Op Chemicals Ltd., Japan). The Na^+ ions (cationic exchange capacity of between 70 and 80 mequiv/100 g) were exchanged with aminododecanoic acid (ADA) as in ref 10.

Preparation. The composites were obtained by compounding the molten polymer with 2, 5, and 10 wt % of organoclay in a Brabender internal mixer (AEV330) at 120 ± 5 °C, 60 rpm for 10 min. The samples are a nanocomposite in the case of MMT-30B and a microcomposite in the case of FH-ADA. The composites were then pressed at 120 ± 5 °C and 100 bar for 2 min to obtain 100 × 100 × 5 mm specimens. Samples of pure polymer were processed in the same way and used for comparison.

Morphological Characterization. Bright-field TEM images of the nanocomposite and the microcomposite were obtained at 80 kV with a Zeiss EM 900 instrument. The samples were cooled at −80 °C and then microtomed with a diamond knife cooled at −60 °C to give sections with a nominal thickness of 50 nm and 1 mm^2 of superficial area. The sections

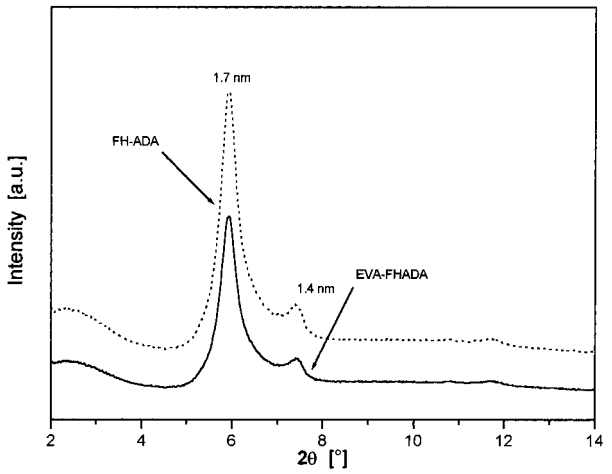

Figure 3. XRD of fluorohectorite exchanged with aminododecanoic acid (FHADA, dotted line) and EVA microcomposite (EVA−FHADA, solid line).

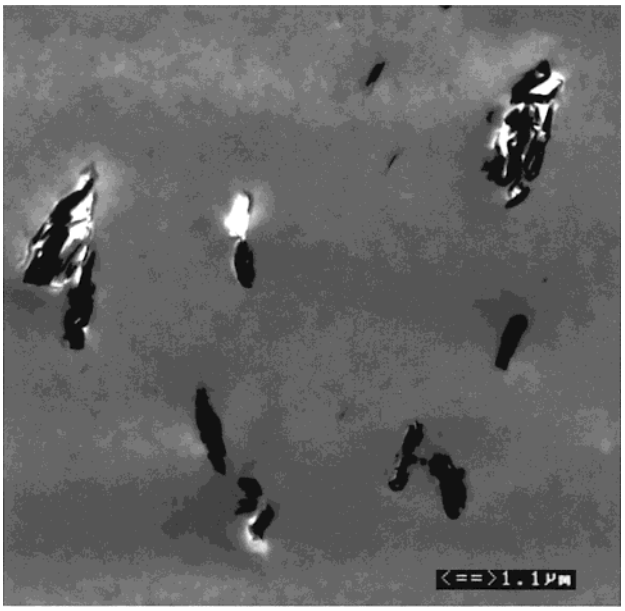

Figure 4. TEM of microcomposite based upon EVA filled with 5 wt % synthetic fluorohectorite exchanged with aminododecanoic acid (EVA19−FHADA).

were collected on the surface of a 60/40 solution of dimethylsulfoxide and water and then transferred to 200-mesh Cu grids.

X-ray diffraction measurements (XRD) were performed on a Philips diffractometer using Co Kα radiation ($\lambda = 0.179$ nm).

Combustion and Thermal Gasification Studies. Combustion experiments were performed in an oxygen consumption calorimeter ("cone calorimeter") at an incident heat flux of 50 kW/m^2.[12] Peak HRR, total heat released, heat of combustion, specific extinction area, CO yield, and CO_2 yield data reproducible to within ±10% when measured at 50 kW/m^2 flux. The cone data reported here are the averages of three replicated experiments.

Gasification experiments[13] were performed in an apparatus similar to the cone calorimeter, built at the NIST, that allows for the pyrolysis, in nitrogen atmosphere, of samples identical to those used in the cone calorimeter at heat fluxes such as those experienced in a fire (30−100 kW/m^2) and is used to

(11) Zilg, C.; Mülhaupt, R.; Finter, J. *Macromol. Chem. Phys.* **1999**, *200*, 661.
(12) Babrauskas, V. *Fire Mater.* **1995**, *19*, 243.
(13) Austin, P. J.; Buch, R. R.; Kashiwagi, T. *Fire Mater.* **1998**, *22*, 221.

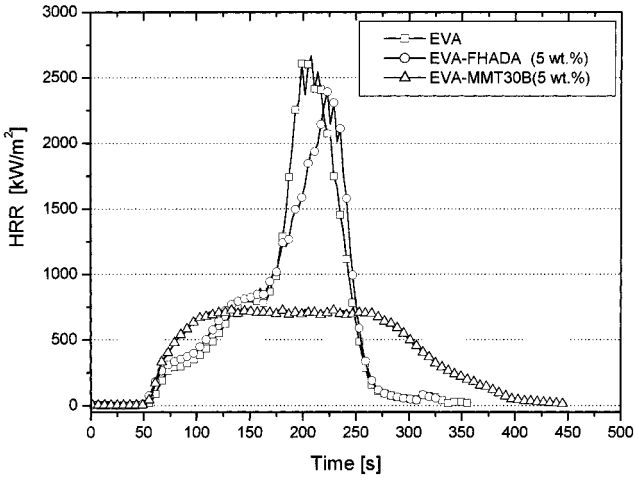

Figure 5. Heat release rate (HRR) plots for pure EVA; EVA with 5 wt % of fluorohectorite exchanged with aminododecanoic acid, a microcomposite; and EVA with 5 wt % of montmorillonite exchanged with methyl, tallow, bis-2-dihydroxyethylammonium, a nanocomposite, at a heat flux of 50 kW/m^2.

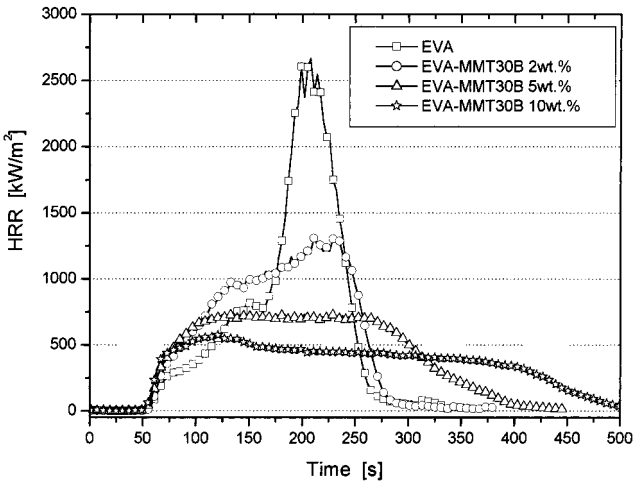

Figure 6. Heat release rate (HRR) plots for pure EVA and EVA filled with 2, 5, and 10 wt % of montmorillonite exchanged with methyl, tallow, bis-2-dihydroxyethylammonium, a nanocomposite, at a heat flux of 50 kW/m^2.

study condensed-phase decomposition processes decoupled from the gas-phase combustion and heat feedback from the flame. A load cell gives mass loss rate data for comparison with the mass loss rate data from the cone calorimeter.

Results and Discussion

Characterization of the EVA−Organoclay Composites. The EVA−MMT30B nanocomposite was given an exfoliated nanomorphology by compounding the molten EVA with methyl, tallow, bis-2-dihydroxyethylammonium-treated montmorillonite (MMT30B). XRD showed the disappearance of the layer spacing of the pristine organoclay (1.82 nm) after compounding (Figure 1) and the appearance of a new reflection peak corresponding to a *d* spacing of 1.5 nm, which might be due to unexchanged Na^+ montmorillonite. The TEM image in Figure 2 shows that the EVA−MMT30B nanocomposite has a mixed morphology. Individual silicate layers are well-dispersed in the polymer matrix, and some tactoids (multilayer particles) composed of two or three layers are also visible.

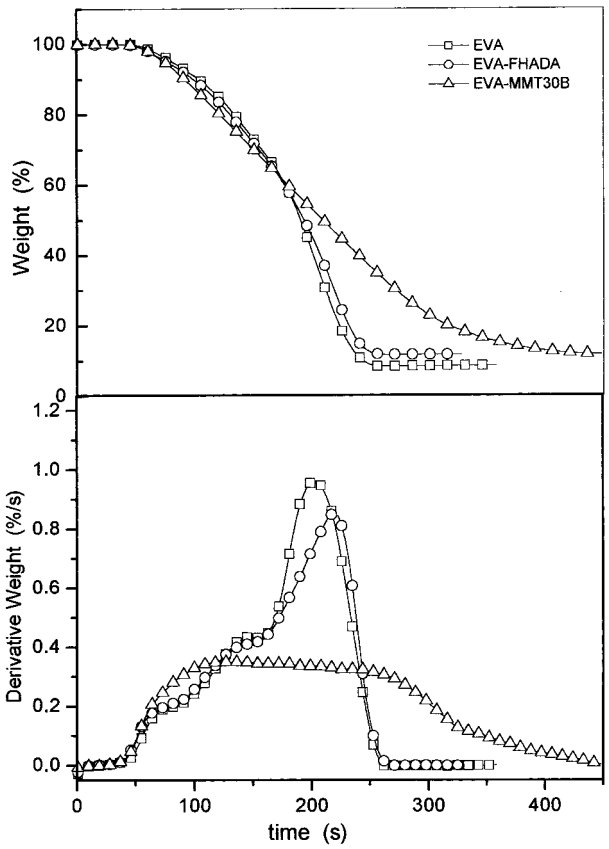

Figure 7. Mass loss rate (MLR) plots for pure EVA; EVA with 5 wt % of fluorohectorite exchanged with aminododecanoic acid, a microcomposite; and EVA with 5 wt % of montmorillonite exchanged with methyl, tallow, bis-2-dihydroxyethylammonium, a nanocomposite, at a heat flux of 50 kW/m^2.

To compare the effect of the nanodispersion of the silicate, a microcomposite (EVA−FHADA) was prepared by compounding the molten EVA with an aminododecanoic acid-treated fluorohectorite (FHADA). When ADA was used for silicate modification, the compatibility of the organoclay and the polymer was poor and insufficient to form the nanocomposite. XRD showed that the silicate dispersed in the polymer matrix retained the stacked structure of the pristine organoclay, with an unaltered *d* spacing of 1.7 nm (Figure 3). The primary particles composed of many silicate layers can be seen in the TEM image of EVA−FHADA (Figure 4). This situation corresponds to that of a conventional filled polymer where primary particles measuring a few microns are dispersed in the matrix.

Combustion and Thermal Gasification. The HRR plots for the nanocomposite, the microcomposite (organoclay mass fraction of 5wt %), and EVA at a 50-kW/m^2 heat flux are shown in Figure 5, The reduction in the peak HRR of the nanocomposite is typical of those reported in the literature.[8,10,14,15] The HRR of the nanocomposite is 78% lower than that of pure EVA and 75% lower than that of the microcomposite. The microcomposite and the nanocomposite display remarkably different combustion behavior. The microcomposite behaves very similarly to the pure polymer. Its peak

(14) Zhu, J.; Morgan, A. B.; Lamelas, F. J.; Wilkie, C. A. *Chem Mater.* **2001**, *13*, 3774.
(15) Zanetti, M.; Camino, G.; Canavese, D.; Morgan, A. B.; Lamelas, F. J.; Wilkie, C. A. *Chem. Mater.*, in press.

Scheme 1

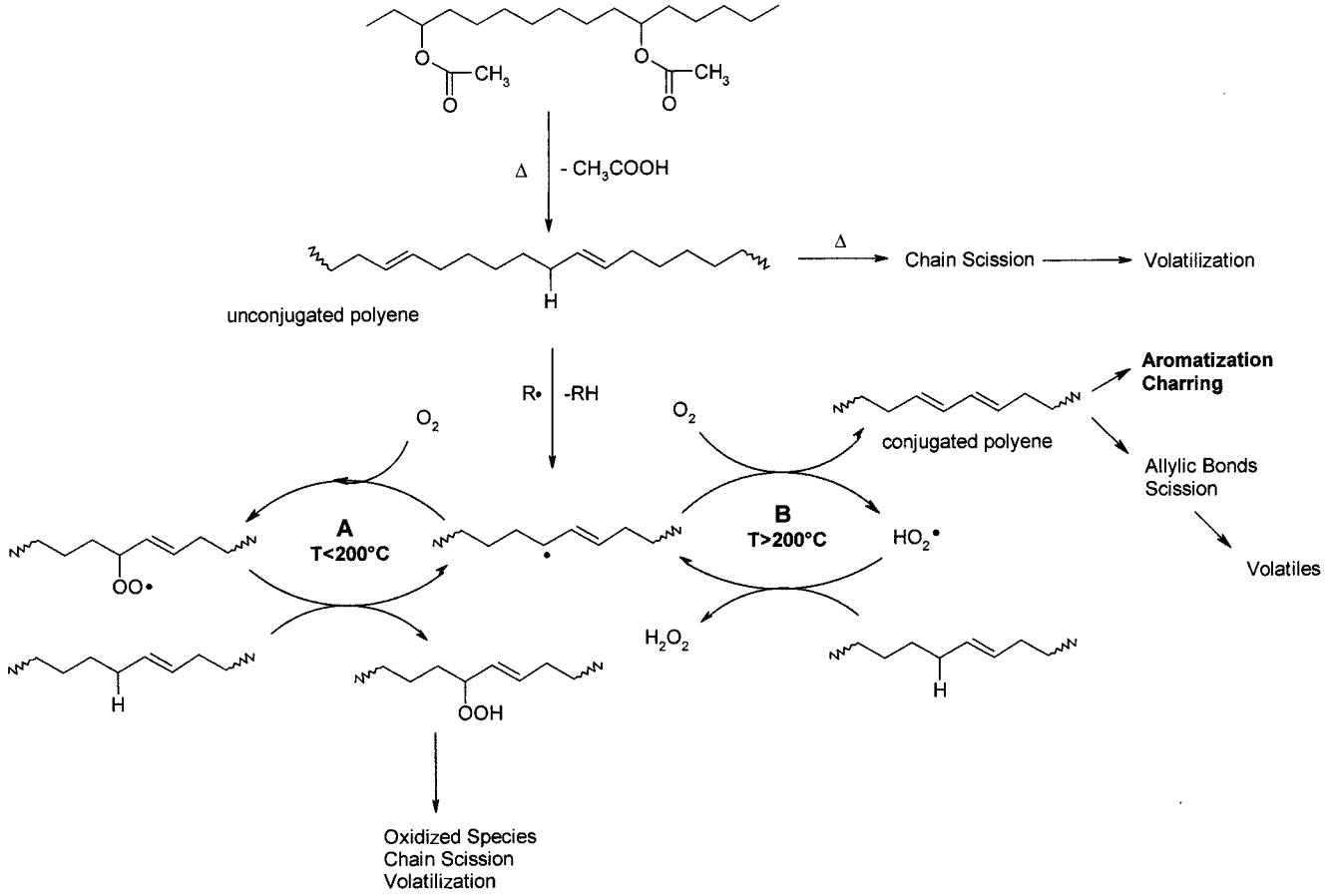

Table 1. Data Recorded in Cone Calorimeter Experiments at a Heat Flux of 50 kW/m^2

sample	total heat released (MJ/m^2)	avg heat of combustion (MJ/kg)	avg specific extinction area (m^2/kg)	CO (kg/kg)	CO_2 (kg/kg)
EVA	202	46	386	0.0329	3.376
EVA + 5 wt % FH	201	49	487	0.0294	3.403
EVA + 2 wt % MMT30B	186	43	668	0.0392	3.240
EVA + 5 wt % MMT30B	179	41	900	0.0445	2.974
EVA + 10 wt % MMT30B	169	39	1040	0.0489	2.773

HRR is lower because it contains 95% EVA. It melts like EVA and has a boiling surface at the base of the flame. The nanocomposite does not melt and chars from the start. At the end of combustion, EVA leaves no residue, and the microcomposite leaves only a little powder. The nanocomposite leaves a solid, consistent char-like residue shaped like the original specimen. The initial HRR for the nanocomposite (Figure 5) is higher for the first minute following ignition (60−125 s from the beginning of the experiment), probably because of thermal decomposition of its organic modifier resulting in the formation of volatile combustibles, as shown in ref 15.

The effect of the MMT30B loading on the HRR is shown in Figure 6. The reduction in the peak HRR increases as the mass fraction of organoclay increases. Figure 7 shows the mass loss and the mass loss rate (MLR) recorded during the cone calorimeter experiment. Because the MLR and HRR curves are very similar, the reduction of the MLR is evidently the primary parameter responsible for the lower HRR of the nanocomposite.

The absence of significant differences in the total heat released, average heat of combustion, specific extinction area, CO yield, and CO_2 yield of EVA and EVA−FHADA (Table 1) indicates that the combustion reaction involved the same degradation products from the polymer. The nanocomposite, on the other hand, displays an 11% total heat released decrease, a 16% heat of combustion decrease, an 85% specific extinction area increase, a 51% CO yield increase, and a 13% CO2 yield decrease, showing that different combustible products reach the flame. In other words, the nanodispersed organoclay changes the polymer's thermal degradation reactions.

Modification of the thermal and thermooxidative behavior of EVA-based nanocomposites was found in ref 16. Thermal degradation of EVA takes place in two stages. In the first, deacetylation with the elimination of acetic acid and the formation of carbon−carbon double bonds in the polymer backbone occurs between 300 and 400 °C. At higher temperatures, thermal degradation of the ethylene-*co*-acetylene random copolymer resulting

(16) Zanetti, M.; Camino, G.; Thomann, R.; Mülhaupt, R. *Polymer* **2001**, *42*, 4501.

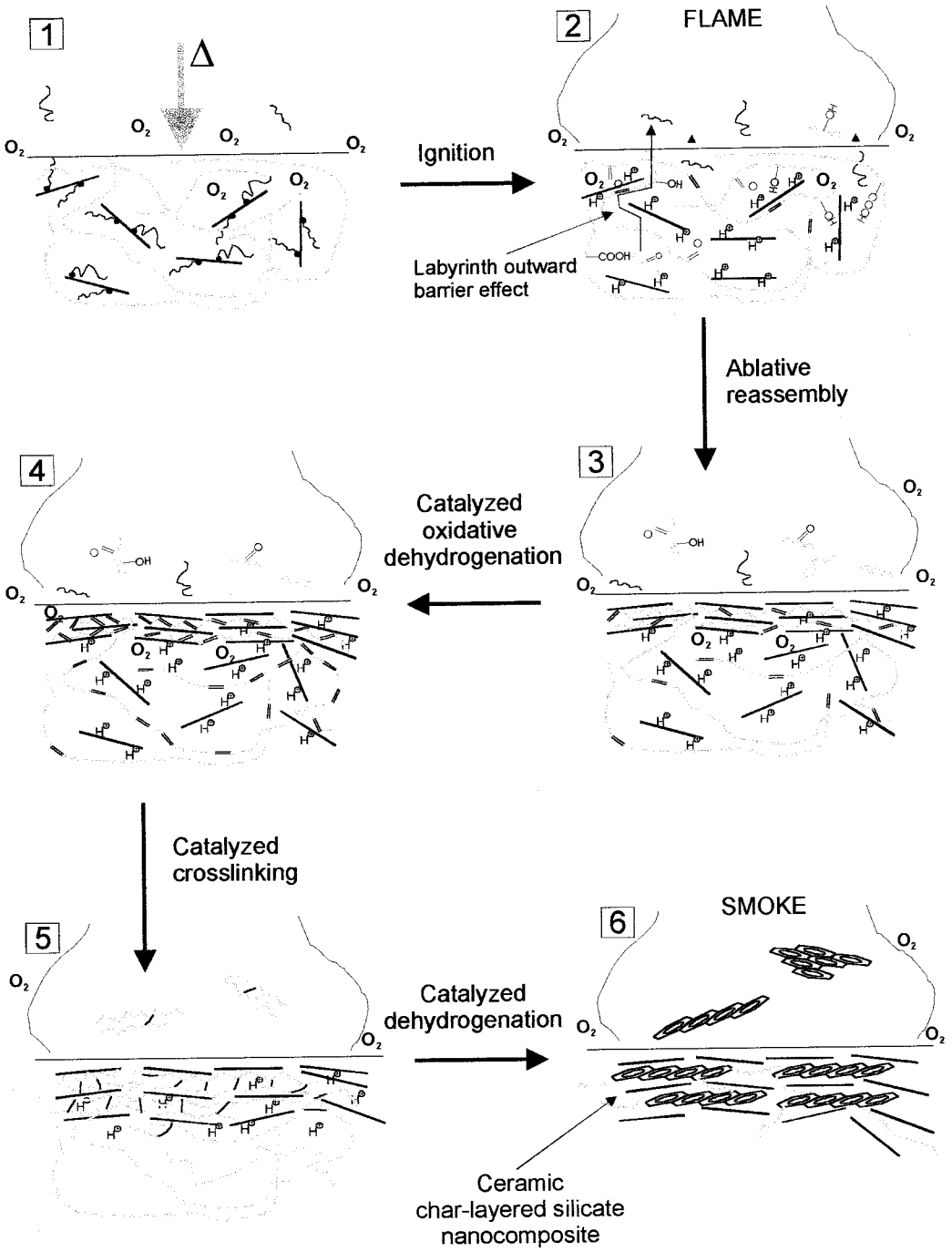

Figure 8. Schematic representation of combustion mechanism and ablative reassembly of a nanocomposite during cone calorimeter experiments.

from deacetylation takes place, with complete volatilization to a mixture of saturated and unsaturated hydrocarbons.[17] Acceleration of the deacetylation reaction is due to a catalytic effect of acidic sites originating from the Hoffman elimination[18] of the organic treatment. Accelerated evolution of acetic acid might contribute to greater heat release in the early stage of nanocomposite combustion compared to combustion of pure EVA.[10] Thermal volatilization of the deacetylated polymer is slowed by the "labyrinth" effect of the silicate layers in the polymer matrix, which lowers the rate of diffusion of the degradation products into the gas phase.[16] The catalytic sites on the silicate surface might also change the thermal degradation reaction of the deacetylated polymer by changing the composition of the volatile products. Furthermore, in air, nanocomposites protect and stabilize against thermooxidation. This property might derive from the barrier produced by the diffusion of oxygen from the gas phase to the polymer. This barrier effect increases during volatilization because of the ablative reassembly of the silicate layers on the polymer surface, which is favored by thermal decomposition of the organoclay.

During combustion, thermal degradation, and thermooxidation of EVA take place following the reactions of Scheme 1. Below 200 °C, radical chain peroxidation

(17) Camino, G.; Sgobbi, R.; Zaopo, R.; Colombier, S.; Scelza, C. *Fire Mater.* **2000**, *24*, 85.

(18) March, J. *Advanced Organic Chemistry*; McGraw-Hill Kogakusa Ltd: Tokyo, 1977; p 927.

process A adds oxygen to the carbon radical created within the polymer chain by hydrogen abstraction.[19] Above 200−250 °C, the in-chain carbon macroradical undergoes preferential hydrogen abstraction by oxygen as in process B, resulting in radical chain oxidative dehydrogenation.[17]

Oxygen is more likely to abstract allylic hydrogen atoms owing to the weaker C−H bond as compared to those in saturated chain segments. Thus, oxidative dehydrogenation leads to conjugated double bond sequences that transform the polyene resulting from deacetylation into a conjugated polyene (Scheme 1, route B), similar to those formed by the thermal deacetylation of poly(vinyl acetate) or the dehydrochlorination of poly(vinyl chloride), which evolve upon heating to aromatized thermally stable charred structures through inter- and intramolecular Diels−Alder reactions.[20]

This charring process is accelerated by the acidic catalytic sites of the layered silicates deriving from Hoffman reaction of the organic alkylammonium cation. The catalytic activity of zeolites (typically alluminosilicates) might depend on the presence of peroxides in their structure.[21] In our case, these peroxides would be generated during heat exposure in air. Thus, charring in the nanocomposites would compete favorably with carbon−carbon polyene backbone scission and lead to volatile chain fragments above 400 °C.[17]

The role of catalysis in charring is indirectly supported by the fact that charring is only effective in the nanocomposite because the intimate contact between the polyene molecules and the atoms of the inorganic crystalline layers is so extensive that thermal bond scission is prevented. In the microcomposite, volatilization prevails over charring because this contact is weak.

The role of oxygen in charring is supported by the fact that only the surface layers of the nanocomposite are charred and thus become an effective ceramic-carbonaceous, thermally stable shield for the polymer, although they also prevent oxygen from diffusing into the bulk to extend its oxidative dehydrogenation carbonizing action. On the other hand, the small amount of oxygen involved in the surface interaction allows this process to take place effectively even in the oxygen-depleted atmosphere on the surface of the burning polymer.

Aromatized charring structures escaping the cross-linking charring by fragmentation to volatile moieties in the charring−volatilization competition might explain the increase of smoke and CO yield in nanocomposite combustion, as it is well-known that unsaturated aromatic compounds burn less easily than the corresponding saturated compounds and produce smoke. These mechanisms are schematically represented in Figure 8.

Heat transfer from an external source or from the flame promotes thermal decomposition of the organoclay and deacetylation of EVA (steps 1 and 2, Figure 8) This results in the creation of protonic catalytic sites on the clay layers that reassemble on the surface of the burning material (step 3). The polyene obtained from EVA deacetylation undergoes competition between peroxidation and chain scission to volatile partially oxidized fragments and catalyzed dehydrogenation and oxidative dehydrogenation (step 4). The resulting conjugated polyene undergoes cross-linking and catalyzed dehydrogenation to form a charred surface layer (step 5), which combines and intercalates with the reassembling silicate layers to provide a sort of ceramic char-layered silicate nanocomposite (step 6).

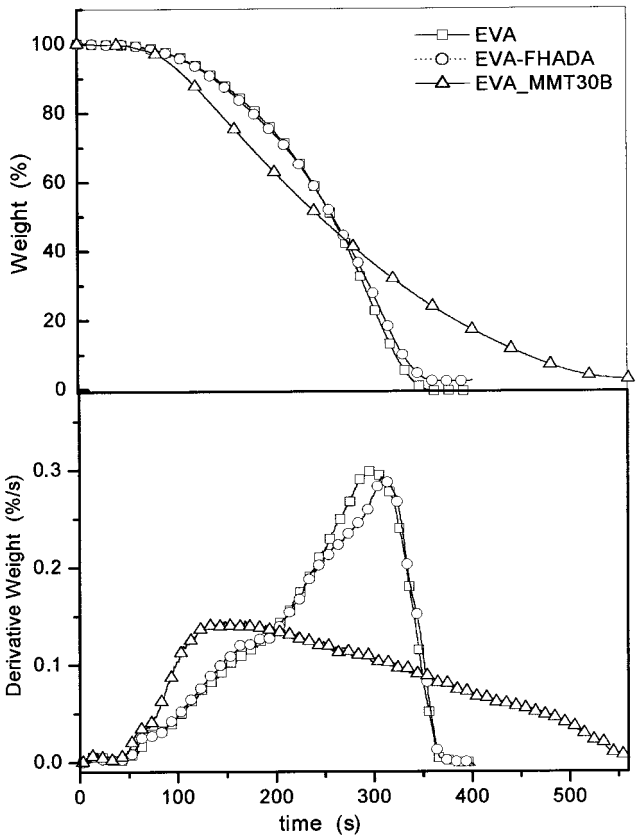

Figure 9. Mass loss rate (MLR) plots for pure EVA; EVA with 5 wt % of fluorohectorite exchanged with aminododecanoic acid, a microcomposite; and EVA with 5 wt % of montmorillonite exchanged with methyl, tallow, bis-2-dihydroxyethylammonium, a nanocomposite, recorded during gasification experiments at a heat flux of 50 kW/m^2.

Owing to the outward−inward labyrinth effect, all of these processes are maximized at the surface of the burning specimen where the concentration of the reacting species is the highest. The carbonaceous silicate structure on the surface might act as an excellent insulator and mass transport barrier that slows the escape of the volatile product generated during decomposition, as was well-explained by Gilman et al.[8] The effect of the nanocomposites in the condensed phase was investigated in experiments performed in a gasification apparatus that allows for pyrolysis in a nitrogen atmosphere of samples identical to those used in the cone calorimeter. Figure 9 shows the mass loss and MLR curves for the samples used in the cone calorimeter experiments of Figures 5 and 7. The EVA and EVA−MMT30B MLR curves display the MLR and HRR trends observed in these experiments. The nanocomposite MLR curve shows not the typical flat shape with a plateau between 100 and 250 s (Figures 5 and 7) but rather a peak corresponding to thermal degradation of the organic modifier of MMT30B, followed by a decreasing

(19) Benson, S. W.; Nogia, P. S. *Acc. Chem. Res.* **1979**, *12*, 233.
(20) Starnes, W. H. *Developments in Polymer Degradation-3*; Applied Science Publishers: Barking, Essex, U.K., 1981; p 152.
(21) Garces, J. M.; Kuperman, A.; Millar, D. M.; Olken, M. M.; Pyzik, A. J.; Rafaniello, W. *Adv. Mater.* **2000**, *12*, 1725.

MLR with a well-defined slope. The gasification residues are similar to those obtained in the cone calorimeter experiments, namely, no residue for EVA, a light-grey powder from the microcomposite, and a charred residue from the nanocomposite.

Both the cone calorimeter and the gasification experiments reveal a small improvement in the carbonaceous char yield, indicating that flame retardancy is mainly due not to retention of a large fraction of fuel in the condensed phase but rather to reduction of the MLR. These data, however, also point to a chemical effect of the nanodispersed silicate that might help to reduce the flammability of the polymer. Additional studies on this chemical effect are underway in our laboratory.

Conclusions

The degree of dispersion and the intercalation spacing of polymer nanocomposites based on organically modified phyllosilicates and EVA prepared by melt processing depend on the type of organoclay. In the case of the montmorillonite clay used here, an exfoliated nanocomposite was obtained, whereas a microcomposite was formed with aminododecanoic acid-exchanged fluorohectorite.

The nanodipersed morphology leads to a substantial decrease of the rate of combustion of the EVA matrix. This is due to surface charring−ceramization, which creates a protective shield for the polymer that slows the flame-feeding thermal decomposition in the nanocomposite, whereas the microcomposite burns in the same way as the pure EVA matrix.

The behavior of the nanocomposite must derive from the morphological control of the shielding properties of the ceramic surface layer created during polymer ablation, which seems to be better when the layer is formed by the reassembly of finely dispersed crystalline silicate layers. On the other hand, the large surface area for clay−polymer contact in the nanocomposite favors catalyzed dehydrogenation and oxidative dehydrogenation of the polymer to a conjugated polyene, which prevents volatilization to combustible volatiles by aromatization and charring. Protonic sites formed on the silicate layers by Hoffman decomposition of the organic modifier of the clay might enhance the catalytic action. Partial volatilization of aromatized polymer structures is responsible for smoke and CO increases during combustion of the nanocomposite

Acknowledgment. The authors thank Alessandro Riva, University of Torino; Jeffry Gilmann, Mike Smith, and John Shields, NIST; Giovanna Costa Imag, CNR; and Rolf Mülhaupt and Carsten Zilg, University of Freiburg, for their helpful contributions.

CM011236K